Aplidin® induces JNK-dependent apoptosis in human breast cancer cells via alteration of glutathione homeostasis, Rac1 GTPase activation, and MKP-1 phosphatase downregulation

L González-Santiago[1,2,7], Y Suárez[1,2,7], N Zarich[3,7],
MJ Muñoz-Alonso[1,2], A Cuadrado[1,2], T Martínez[1], L Goya[4],
A Iradi[5], G Sáez-Tormo[5], JV Maier[6], A Moorthy[6], ACB Cato[6],
JM Rojas[3] and A Muñoz*,[1]

[1] Instituto de Investigaciones Biomédicas 'Alberto Sols', Consejo Superior de Investigaciones Científicas-Universidad Autónoma de Madrid, Arturo Duperier, 4, Madrid E-28029, Spain
[2] Pharma Mar S.A., E-28770 Colmenar Viejo, Madrid, Spain
[3] Centro Nacional de Microbiología, Instituto de Salud Carlos III, Carr. Majadahonda-Pozuelo Km 2, E-28220 Majadahonda, Madrid, Spain
[4] Instituto del Frío, Consejo Superior de Investigaciones Científicas, José Antonio Novais 10, Madrid E-28040, Spain
[5] Facultad de Medicina, Universidad de Valencia, Avda. Blasco Ibáñez 17, Valencia E-46001, Spain
[6] Forschungszentrum Karlsruhe, Institute of Toxicology and Genetics, Karlsruhe D-76021, Germany
[7] These authors contributed equally to this work.
* Corresponding author: A Muñoz, Molecular Endocrinology, Instituto de Investigaciones Biomédicas 'Alberto Sols', Arturo Duperier, 4, E-28029 Madrid, Spain. Tel: +34 91 585 4451; Fax: +34 91 585 4401; E-mail: amunoz@iib.uam.es

Abstract

Aplidin® is an antitumor agent in phase II clinical trials that induces apoptosis through the sustained activation of Jun N-terminal kinase (JNK). We report that Aplidin® alters glutathione homeostasis increasing the ratio of oxidized to reduced forms (GSSG/GSH). Aplidin® generates reactive oxygen species and disrupts the mitochondrial membrane potential. Exogenous GSH inhibits these effects and also JNK activation and cell death. We found two mechanisms by which Aplidin® activates JNK: rapid activation of Rac1 small GTPase and downregulation of MKP-1 phosphatase. Rac1 activation was diminished by GSH and enhanced by L-buthionine (SR)-sulfoximine, which inhibits GSH synthesis. Downregulation of Rac1 by transfection of small interfering RNA (siRNA) duplexes or the use of a specific Rac1 inhibitor decreased Aplidin®-induced JNK activation and cytotoxicity. Our results show that Aplidin® induces apoptosis by increasing the GSSG/GSH ratio, a necessary step for induction of oxidative stress and sustained JNK activation through Rac1 activation and MKP-1 downregulation.
Cell Death and Differentiation (2006) **13,** 1968–1981.
doi:10.1038/sj.cdd.4401898; published online 17 March 2006

Introduction

Aplidin® is an antitumor compound in Phase II clinical trials against a variety of tumors. Chemically, it is a cyclic depsipeptide originally isolated from the marine tunicate *Aplidium albicans* and currently obtained by total synthesis.[1] Aplidin® is an extremely potent inducer of apoptosis, with IC_{50} in the low nanomolar range, of many tumor cell types *in vitro*,[2–4] and it also exhibits strong antitumor activity in xenograft models.[5]

The mechanism of action of Aplidin® is only partially understood. It induces apoptosis via caspase-dependent and -independent mechanisms irrespective of the p53 tumor suppressor status and without affecting the cell cycle phases.[4,6–8] In human breast MDA-MB-231, cervical HeLa and several renal cancer cells Aplidin® causes a rapid and sustained increase in the phosphorylation of epidermal growth factor receptor (EGFR) and the activation of the kinases Src, Jun N-terminal kinase (JNK) and p38 mitogen-activated protein kinase (MAPK).[4,9] These effects are attenuated by addition of exogenous reduced glutathione (L-γ-glutamyl-L-cysteinylglycine, GSH) or Ebselen or N-acetylcysteine, both of which raise the cellular content of GSH. In HeLa cells, Aplidin® also induces extracellular signal-regulated kinase (ERK) and protein kinase C-δ, and rapidly induces the apoptotic mitochondrial pathway thus promoting cytochrome c release from the mitochondria and caspase-3 activation.[9] By using a series of inhibitors and several genetically deficient mouse embryo fibroblasts (MEF) we showed that JNK activation precedes that of EGFR and is critical for apoptosis induction by Aplidin®.[10] Data indicated that the phosphorylation by JNK of c-Jun and other unknown substrates is crucial for Aplidin® cytotoxicity.[10] Aplidin® rapidly induces a series of genes of the *JUN* and *FOS* families, and p65/*RELA* in MDA-MB-231 cells, which leads to a transient increase in activator protein (AP)-1 and nuclear factor *kappa* B (NFκB) activity.[10] However, the role of these transcription factors in the induction of apoptosis remains to be established.

The action of Aplidin® in human hematopoietic cells such as T-lymphoid Jurkat, promyelocytic HL-60 and erythroleukemic HEL cell lines has also been studied. In these cells, Aplidin® also activates JNK, and promotes both the mitochondrial and the Fas/CD95 receptor apoptotic pathways.[11] In leukemic MOLT-4 cells, Aplidin® inhibits growth and induces apoptosis through the blockade of the vascular endothelial growth factor (VEGF)/VEGF receptor-1 autocrine loop via the inhibition of VEGF secretion.[12] In line with this, Aplidin® is anti-angiogenic by inhibiting VEGF- and fibroblast growth factor-2-induced endothelial cell functions (proliferation, migration, invasiveness).[13] However, Aplidin® inhibited VEGF secretion only in one out of four lines derived from patients with acute lymphoblastic leukaemia, and this effect was unrelated to its cytotoxicity.[14]

In conditions of maximal growth stimulation in vitro no differences in drug sensitivity have been observed between normal and tumoral cells. However, non-tumoral human cells were more sensitive to Aplidin® upon growth-stimulation than in serum-starvation. This difference, which is not seen in tumoral cells probably because of their autocrine stimulation, is reflected in higher activation of JNK.[10]

Here we examine the molecular mechanism of induction of apoptosis by Aplidin® in MDA-MB-231 cells focusing on two aspects: the importance of GSH and the mechanism of JNK activation. First, we show that Aplidin® alters cellular glutathione homeostasis thus increasing the ratio of oxidized (GSSG) to reduced (GSH) forms (GSSG/GSH) by altering several mechanisms of glutathione control. Our data indicate that this effect is essential for the induction of apoptosis, and leads to increases in levels of reactive oxygen species (ROS) and lipid and DNA oxidation. Second, we report that Aplidin® induces rapid, transient and GSH-dependent stimulation of

the Rac1 small GTPase, upstream activator of JNK in several cell types. Rac1 activation plays an important role in JNK activation as both Rac1 downregulation by transfection of siRNA duplexes specific for Rac1 and the co-treatment with a specific inhibitor of Rac1 activity consistently diminished JNK activation and apoptosis induction by the drug. Moreover, Aplidin® decreases the cellular level of MKP-1, a major phosphatase inactivating JNK, with kinetics compatible with the sustained activation of JNK observed in drug-treated cells.

Results

GSH is crucial for Aplidin® cytotoxicity

First, we studied the effects of a series of antioxidants on the induction by Aplidin® of EGFR and JNK/p38MAPK phosphorylation and apoptosis. Only Ebselen and NAC, which increase cellular GSH levels, inhibited EGFR and JNK/p38MAPK activation (Table 1). Aplidin®-induced apoptosis was also inhibited by Ebselen, and to a lesser extent by thiourea, whereas longer treatments with NAC were cytotoxic. In contrast, BSO, an inhibitor of the γ-glutamylcysteine synthetase required for GSH synthesis, increased Aplidin®-induced kinase activities and apoptosis. These results pointed to GSH as a crucial mediator of Aplidin® action. Moreover, exogenous GSH prevented the loss of mitochondrial membrane potential (ΔΨm) caused by Aplidin® as estimated by flow cytometry using JC-1: the drug caused an increase in the green and a decrease in the red fluorescence that was blunted by GSH (Figure 1a). Furthermore, exogenous GSH also reduced cell death caused by the drug (Figure 1b).

Table 1 Effect of different antioxidants on Aplidin® action

Compound	Proposed mechanism of action	Aplidin® action		
		EGFR activation	JNK p38 Activation	Apoptosis induction
Catalase	Conversion of H_2O_2 into H_2O+O_2	No	No	No
CuZn SOD	Dismutation of O_2^- radical anion	No	No	No
MnSOD	Dismutation of O_2^- radical anion	No	No	No
Mn(III)TMPyP	SOD mimetic	Not done	Not done	No
Ascorbic acid	General antioxidant	No	No	Not done
Tiron	Intracellular superoxide scavenger	No	No	G1 arrest
DPI	Inhibitor of NAPDH oxidase	No	No	Cytotoxic
Thiourea	Radical hydroxyl scavenger	Not done	No	Decrease
Ebselen	NADPH oxidase, 5-LO and COX inhibitor, peroxides scavenger, glutathione peroxidase mimetic	Decrease	Decrease	Decrease
NAC	ROS scavenger, glutathione precursor	Decrease	Decrease	Cytotoxic
BSO	Reduction of intracellular GSH levels	Increase	Increase	Not done
L-NAME	Nitric oxide synthesis inhibitor	No	No	No
Sper-NO	Nitric oxide donor	No	No	No

MDA-MB-231 cells were incubated overnight with the indicated antioxidants before addition of Aplidin (500 nM). EGFR activation was analyzed by coupled immunoprecipitation and Western blotting using antI-EGFR and anti-phosphotyrosine antibodies, respectively. JNK and p38 MAPK activation was analyzed by Western blotting using anti-phospho-JNK and anti-phospho-p38 MAPK antibodies. Anti-total JNK and p33 MAPK antibodies were used for normalization. *Increase* and *Decrease* mean 50% elevation or reduction as compared to cells incubated with vehicle before addition of Aplidin in at least three independent experiments. *No* means that change caused by pretreatment with the antioxidant was less than 50%. Apoptosis induction was analyzed by flow cytometry 24 h after Aplidin addition. *G1 arrest* or *Cytotoxic* mean that the antioxidant itself induced substantial (>30%) accumulation of cells in G1 phase or the hypodiploid subG1 peak, respectively. *Decrease* means that pretreatment with the antioxidant diminished >30% the hypodiploid peak induced by Aplidin. *No* means that the effect was smaller than 30%. Three independent experiments were done in every case
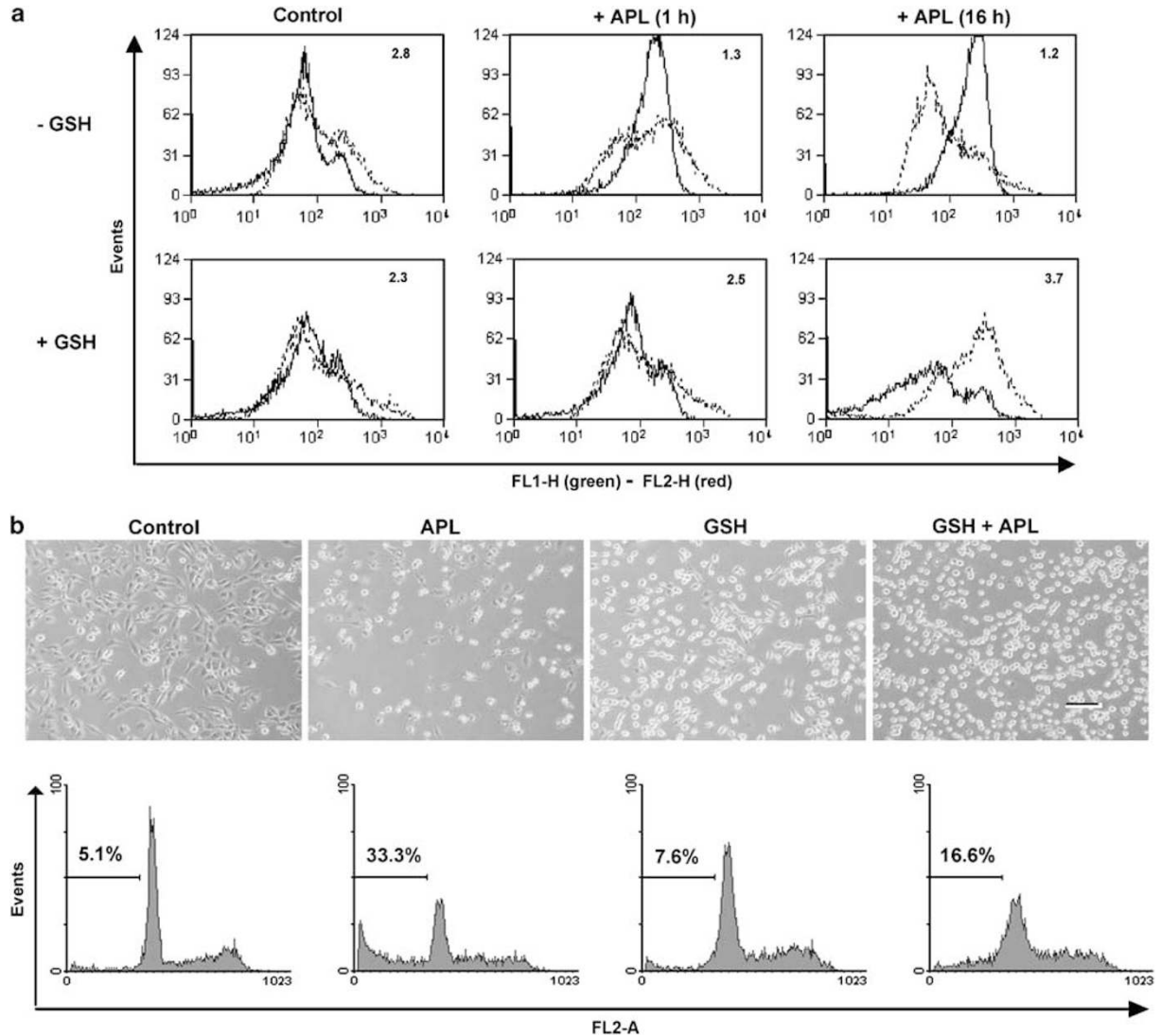
Figure 1 Aplidin® disrupts the mitochondrial membrane potential ($\Delta\Psi$m) and GSH reverts $\Delta\Psi$m loss and cell death induced by Aplidin®. (**a**) Flow cytometry analysis of MDA-MB-231 cells incubated with 500 nM Aplidin® for the indicated times or left untreated (control) and then stained with JC-1 as described in Materials and methods. Cells treated with 10 μM valinomycin for 2 h were used as control of depolarisation (data not shown). Abscissas show FL1-H (green fluorescence, continuous lane) and FL2-H (orange-red fluorescence, discontinuous lane) values. Data correspond to a representative experiment out of three that gave similar results. Numbers refer to the ratio of red/green fluorescence. (**b**) Phase-contrast micrographs (upper part) and flow cytometry analysis of DNA content (lower part) of cells treated with vehicle (Control), 500 nM Aplidin® (APL), 0.5 mM GSH or both (GSH added 30 min before Aplidin® for 48 h). Scale bar, 25 μm. Percentages of apoptotic cells corresponding to the subdiploid population are shown

Aplidin® increases the GSSG/GSH ratio and induces oxidative stress

Next, we examined the effect of Aplidin® on cellular glutathione homeostasis, by measuring the levels of GSH and GSSG in MDA-MB-231 cells. Aplidin® induced a decrease in GSH and an increase in GSSG levels, thus raising the GSSG/GSH ratio (Figure 2a). This effect was blocked by Ebselen. Given the crucial role of glutathione in the control of the cellular redox status, the increase in GSSG/GSH ratio suggested the generation of oxidative stress. Indeed, we found a progressive increase by Aplidin® of the cellular content of malondialdehyde, a marker of membrane phospholipid oxidation, which was prevented by BHA, an

inhibitor of lipoperoxidation (Figure 2b). Likewise, Aplidin® increased the level of 8-oxo-2′-deoxyguanosine, a marker of DNA oxidation (Figure 2c). Further supporting the induction of oxidative stress, overexpression of exogenous thioredoxin, the second major cellular antioxidant system together with GSH, decreased the level of JNK activation by Aplidin® (Figure 2d). Moreover, by incubating the cells in phosphate-buffered saline (PBS) we found that Aplidin® induced the extrusion of GSH to the extracellular medium (Table 2). To study the effect of GSH extrusion, we examined the effect of inhibitors of plasma membrane GSH transport: L-methionine and L-cystathionine, of the sinusoidal system, and BSP, of the canalicular system. All three compounds decreased JNK activation and cell death by Aplidin® (Figure 3). We also
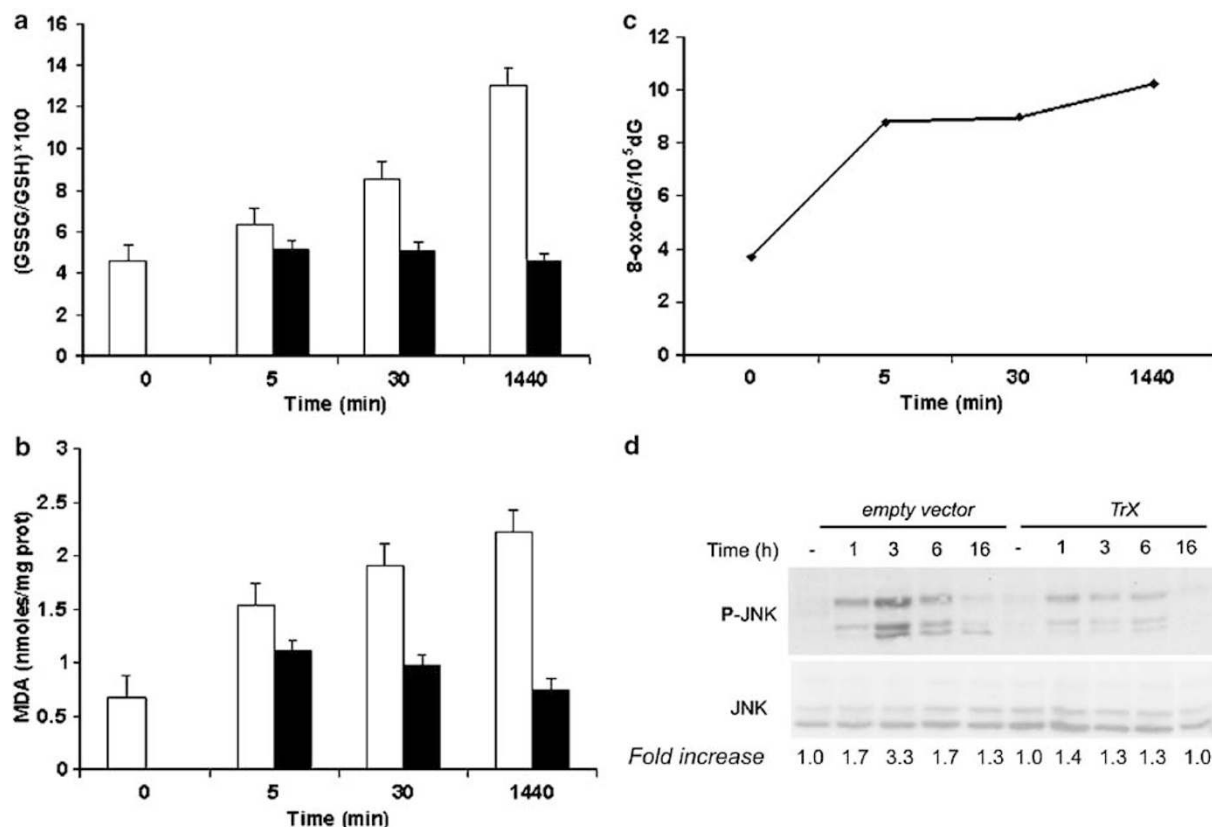
Figure 2 Aplidin® increases the GSSG/GSH ratio and induces oxidative stress in MDA-MB-231 cells. (**a**) Ratio of the levels of GSSG and GSH measured as described in Materials and methods in cells treated with 500 nM Aplidin® in the absence (white columns) or presence (black columns) of 40 μM Ebselen for the indicated times. (**b**) Levels of malondialdehyde (MDA) measured as described in Materials and methods in cells treated with 500 nM Aplidin® in the absence (white columns) or presence (black columns) of 100 μM BHA for the indicated times. (**c**) Levels of 8-oxo-2'-deoxyguanosine (8-oxo-dG) measured as described in Materials and methods in cells treated with 500 nM Aplidin® for the indicated times. (**d**) Effect of overexpression of exogenous thioredoxin (TrX) on the activation of JNK by Aplidin®. Levels of activated JNK in cells that were transfected with an empty vector or a TrX expression vector as described in Materials and methods at the indicated times of Aplidin® treatment (500 nM) initiated 24 h after transfection were measured by Western blot using phospho-specific antibodies (P-JNK). An antibody against total JNK protein was used to rule out effects at the expression level. Numbers refer to fold-increase activation with respect to untreated (−) cells

Table 2 GSH extrusion upon Aplidin® treatment

	Protein (nmol/mg)	% Control
Control	79.7 ± 8.6	100
APL, 5 min	61.7 ± 12.4	77.4
APL, 30 min	94.1 ± 1.5	118.1
APL, 1440 min	126.1 ± 17.9	160.7
Exog. GSH	394.8 ± 31.1	495.3

GSH secreted by cells treated with 500 nM Aplidin (APL) or left untreated (control) for the indicated times was measured as described under Materials and Methods. As an additional control, a solution of 0.5 mM GSH was used (Exog. GSH)

studied the effect of Aplidin® on the enzymes responsible for GSSG-GSH interconversion. Aplidin® induced a rapid, strong but transient inhibition of GPx activity, and a later decrease in GR, which may contribute to the disruption of glutathione homeostasis (Figure 4). In line with these data, Aplidin® increased the cellular levels of ROS as measured by flow cytometry using 2',7'-DCFH-DA, an effect that was largely prevented by exogenous GSH treatment (Figure 5a).

Early GSH depletion and loss of mitochondrial function are associated with later changes in ROS generation and disruption of Ca^{2+} homeostasis in some apoptotic systems.[15] We studied the effect of Aplidin® on intracellular Ca^{2+} levels in two conditions. First, we found a rapid transient decrease in intracellular Ca^{2+} when cells were labeled with Fluo-4 and treated with Aplidin® in normal Ca^{2+}-containing growth medium (Figure 5b, left part). Ca^{2+} levels progressively normalized and reached higher levels at 1 h post-treatment concomitantly with an increase in cell membrane permeability revealed by a decrease in FDA fluorescence, suggesting that the recovery may be attributable to Ca^{2+} influx from the extracellular medium. At this early time, no incorporation of PI was detected. Second, when cells were treated with Aplidin® in normal growth medium, washed and then labeled in Ca^{2+}-free medium intracellular Ca^{2+} levels decreased and did not recover for 10 h (Figure 5b, right part). These data do not support a major role of Ca^{2+} in Aplidin® action.

We also examined whether Cu^{2+}, a pro-oxidant agent that mediates neuronal cell death induced by GSH depletion in neurons,[16] affected Aplidin® action. Cu^{2+} enhanced Aplidin® cytotoxicity (Table 3) and JNK activation (data not shown). Both effects were blocked by bathocuproinedisulfonic acid (BCPS), a Cu^{2+} chelating agent. However, BCPS alone did not inhibit Aplidin® cytotoxicity, indicating that Cu^{2+} does not
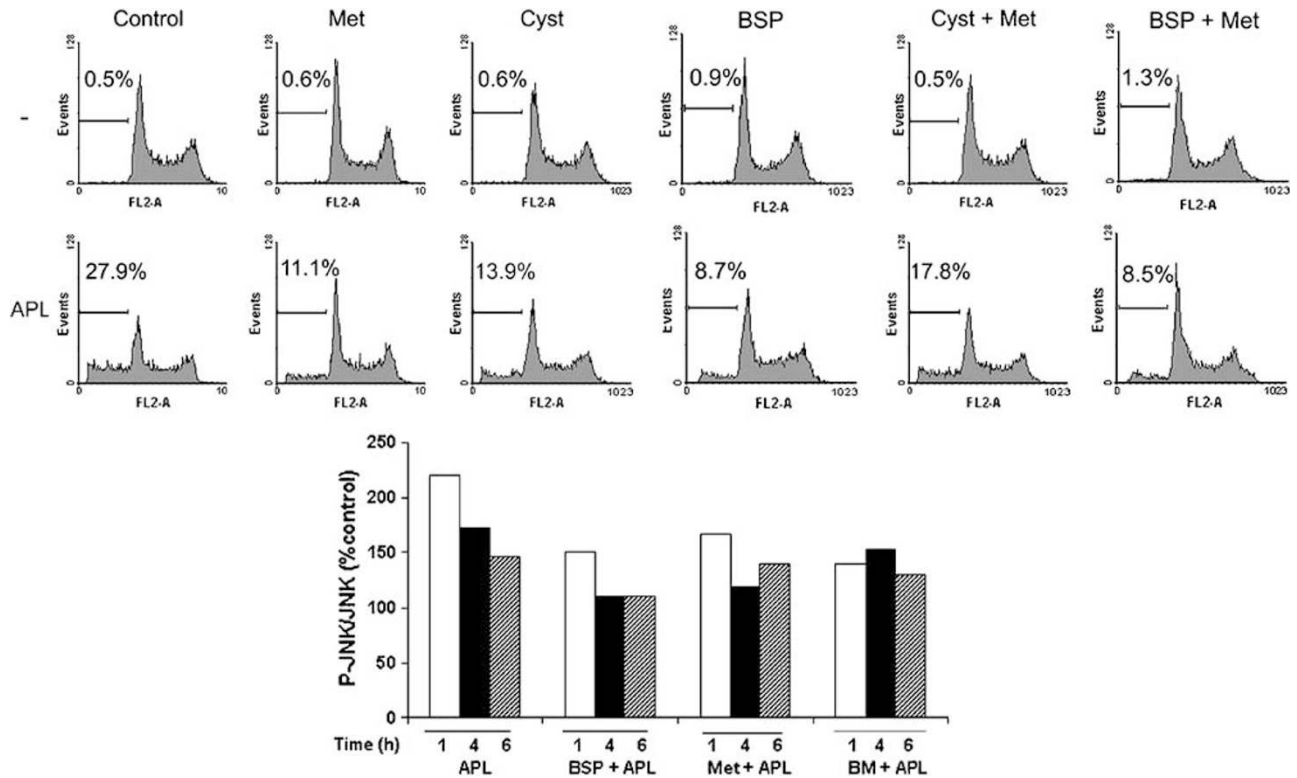
Figure 3 Effect of inhibitors of GSH transport systems on the induction of JNK activation and apoptosis by Aplidin® in MDA-MB-231 cells. Cells were treated with 1 mM L-methionine (Met), L-cystathionine (Cyst), bromosulfophthalein (BSP), or their combinations 1 h before addition of vehicle (control) or 500 nM Aplidin® (APL). Upper part, flow cytometry analysis at 24 h post-treatment. Percentages of apoptotic cells corresponding to the subdiploid population are shown. Lower part, quantification of JNK activation (normalized to total JNK levels) at the indicated times post-treatment

mediate Aplidin® action (Table 3). The possibility that GSH could interact directly with the drug and block its cytotoxic activity was ruled out in experiments in which GSH and Aplidin® were pre-incubated together before addition to MDA-MB-231 cells. In such conditions we found the same level of inhibition of JNK activation and cell death as when cells were pretreated with GSH for 30 min and then with the drug (data not shown).

As GSH depletion induces cell death via activation of phospholipase A2 (PLA2) and lipoxygenases (LPO) in some neuronal populations,[17] and also activates a 12-LPO in epithelial cells,[18] we explored the effect of the inhibition of these enzymes on Aplidin® action. However, neither ATK (arachidonyl-L-trifluoromethylketone), a PLA2 inhibitor, nor baicalein (12-LPO inhibitor), 5,6-dehydro-arachidonic acid (15-LPO inhibitor) nor 12-nordihydroguaiaretic acid (a general LPO inhibitor) significantly affected Aplidin®-induced Jun N-terminal kinase activation or apoptosis (data not shown). Likewise, RHC-80267/U-57908, an inhibitor of diacylglycerol kinase, which is another source of arachidonic acid in addition to PLA2, also failed to modulate Aplidin® action. These results indicate that neither PLA2 nor LPO plays a major role in Aplidin® action.

Next, we examined whether Aplidin® affected the interaction between JNK and glutathione S-transferases (GST)-π1π2. These proteins bind JNK and inhibit its activity acting as monomers in normal cell conditions and are released from JNK to form dimers under oxidative stress conditions.[19] As expected, the induction of JNK phosphorylation and cell death by Aplidin® was higher in cells deficient for GST-π1/π2 than in wild-type MEF. In line with this, Aplidin® promoted the rapid and transient formation of dimers in wild-type fibroblasts (not shown). However, by coupled immunoprecipitation and Western blotting we found that Aplidin® did not affect the interaction of JNK with glutathione-S-transferase (GST)-π1/π2 in MDA-MB-231 cells (not shown), which indicates that these enzymes do not mediate Aplidin® action.

Aplidin® activates the Rac1 small GTPase and downregulates MKP-1 phosphatase

JNK is activated by oxidative stress and other stimuli in various cell types through mechanisms that are not fully understood.[20–23] We examined whether the activation of JNK by Aplidin® was a direct effect on the enzyme or the indirect result of the modulation of upstream regulator(s). We studied the activity of Ras, Rho and Rac1 small GTPases, which activate JNK in many biological systems.[24–26] We found that the drug consistently induces a rapid increase in the Rac1, but not Ras or Rho, activity in HeLa cells (Figure 6a, and data not shown). The cellular content of Rac1 was unchanged. The activation of Rac1 by Aplidin is not specific to HeLa cells, as it was also found in human MDA-MB-231 breast and LS174-T colon cells and in MEF (Figure 6b). Moreover, Rac1 activation by the drug was also found in JNK-deficient (jnk1/2−/−) MEF,
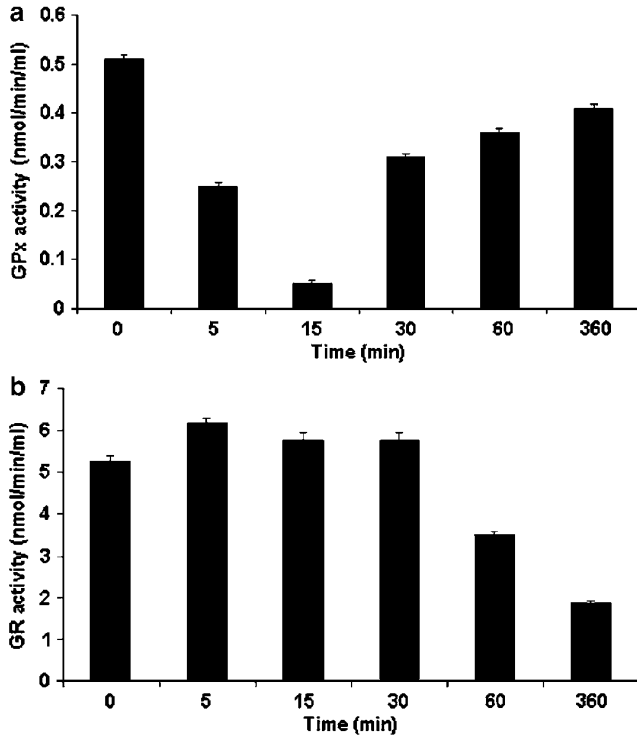
Figure 4 Aplidin® alters GPx (a) and GR (b) activity, respectively, in extracts of MDA-MB-231 cells following Aplidin® treatment measured as described in Materials and methods. Two independent experiments using triplicates were done. Mean values and standard deviations are shown

indicating that it precedes and does not require JNK activity (Figure 6b). This conclusion is also suggested by the analysis of the kinetics of Rac and JNK activation in Hela (Figure 6a), wild-type MEF and MDA-MB-231 (Figure 6b) cells, and by the finding that SB203580, an inhibitor of p38 MAPK and JNK in MDA-MB-231 cells,[4] did not prevent Rac activation by Aplidin® (not shown). The activation of Rac1 was dependent on GSH depletion, as it increased in the presence of BSO and decreased with exogenous GSH (Figure 6c).

To assess the involvement of Rac1 in Aplidin®-promoted JNK activation, we transfected MDA-MB-231 and HeLa cells with two siRNA covering different Rac1 sequences (Rac1.1

Table 3 Role of Cu^{2+} in Aplidin®-induced apoptosis in MDA-MB-231 cells

Treatment	% Apoptotic cells
Single	
Control	1.7
APL, 500 nM	19.6
Cu^{2+}, 8 μM	2.5
BCPS, 300 μM	1.9
Combined	
APL+Cu^{2+}	27.2
APL+BCPS	20.1
APL+Cu^{2+}+BCPS	16.3
Cu^{2+}+BCPS	2.3

Cells were treated with the indicated concentrations of Aplidin (APL), Cu^{2+} and/ or BCPS. Percentages of apoptotic cells were measured 24 h later by flow cytometry
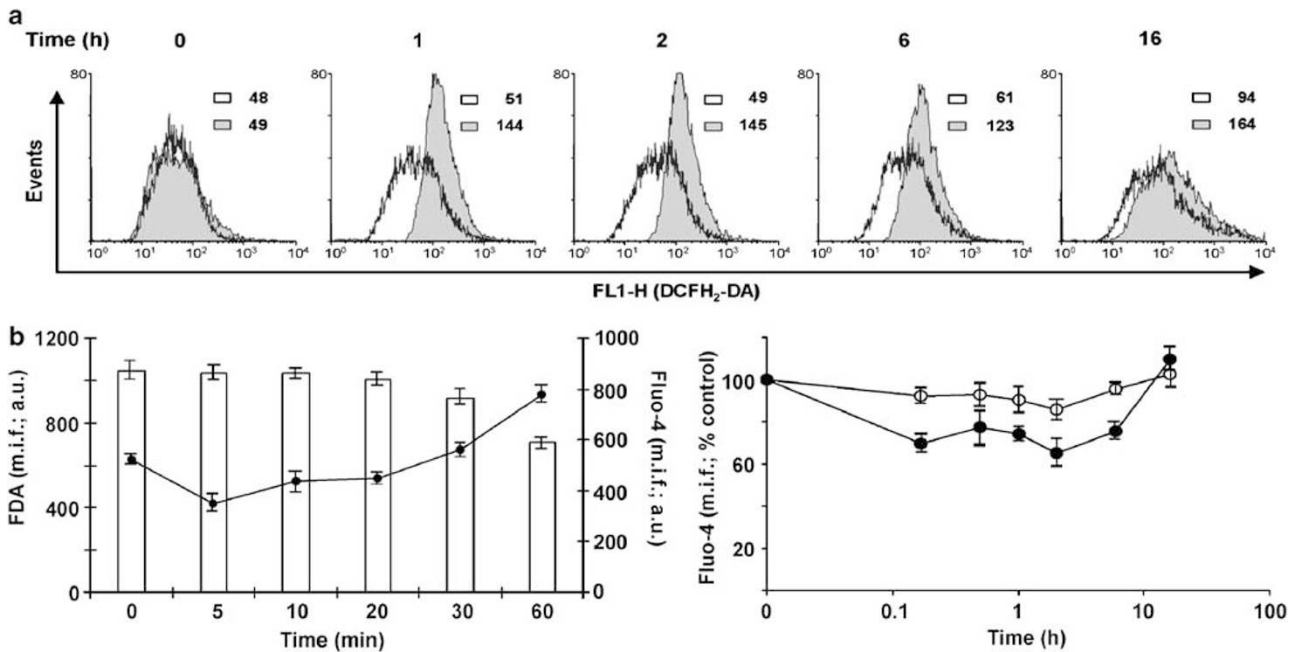
Figure 5 Aplidin® increases cellular ROS and Ca^{2+} levels. (a) ROS levels in MDA-MB-231 cells treated with 500 nM Aplidin® in the absence (solid histograms) or presence (open histograms) of 0.5 mM GSH for the indicated times were measured by flow cytometry as described in Materials and methods. Numbers refer to mean of fluorescent intensity (arbitrary units) of each histogram. (b) effect of Aplidin® on intracellular Ca^{2+} levels. Left part, short kinetics of changes in cellular Ca^{2+} levels (circles) and membrane permeability (columns) upon Aplidin® treatment measured both as described in Materials and methods. Right part, long kinetics of Ca^{2+} content of cells treated with 500 nM Aplidin® (solid circles) or left untreated (open circles)
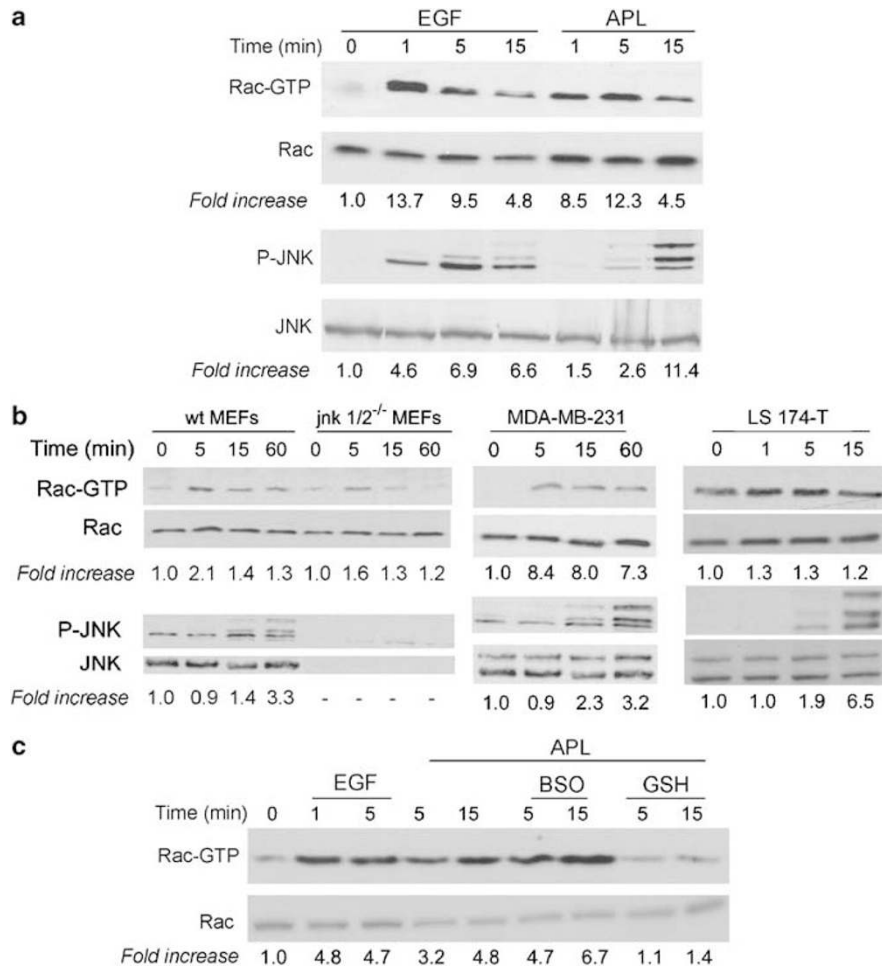
Figure 6 Aplidin® induces activation of the Rac1 GTPase. (**a**) HeLa cells were serum-starved for 18 h and then incubated with EGF (100 ng/ml) or Aplidin® (500 nM) for the indicated times. Left, Rac1-GTP was recovered from cell lysates by binding to immobilized GST-PAK-CRIB and detected by Western blot with anti-Rac1 antibody. The expression levels of the endogenous Rac1 was detected by Western blot of the cell extracts with anti-Rac1 monoclonal antibody. Likewise, the levels of phosphorylation of JNK were determined using specific anti-phospho- and -total JNK antibodies. Values of Rac and JNK activation were normalized to those of total Rac and JNK protein levels of each sample as determined by Western-blot analysis. Mean fold-increase values of Rac-GTP and phospho-JNK obtained in three independent experiments are shown. (**b**) Rac activation by Aplidin® in human MDA-MB-231 and LS174-T cells and in wild-type and *jnk1/2*[−/−] MEF. Rac1 activity and JNK activation were estimated as in (**a**). (**c**) Effect of GSH and BSO on the activation of Rac1 by Aplidin®. HeLa cells were pretreated with 0.5 mM GSH (30 min) or 1 mM BSO (overnight) before Aplidin® addition. Rac1 activity was estimated as in (**a**). Mean values obtained in two independent experiments are shown

and Rac1.3) or with a mixture of siRNA oligonucleotides (D-Mix) (see Materials and methods for details). Western blotting on Rac siRNA transfectant lysates revealed a clear decrease in Rac1, whereas Rac expression levels similar to those found in non-transfected cells were detected using control siRNA (Figure 7a and b, upper left panels). Decreased Rac expression in Rac1.1, Rac1.3 and D-Mix siRNA transfectants correlated with a reduction of JNK activation by Aplidin® as compared with activation exhibited by control siRNA transfectants (Figure 7a and b, upper right and lower panels). Total JNK and β-tubulin protein levels were unaffected by siRNA transfection. Next we studied the effect of Rac1 downregulation on Aplidin®-induced apoptosis. To this end, MDA-MB-231 and Hela cells were co-transfected with either Rac1 or control siRNA and an additional fluorochrome (FAM)-labeled unrelated siRNA. This allowed us to analyse, by flow cytometry, the effect of drug treatment specifically in transfected cells. In addition, a parallel series of plates were

transfected with β-actin siRNA instead of Rac1 siRNA for further control. The analysis of early (annexin V) and late (PI) labeling markers showed that Rac1 siRNA decreased apoptosis induction by Aplidin® (Table 4). Transfection of β-actin siRNA had no effect (not shown).

To further examine the role of Rac1 activation in Aplidin® action, we used a specific Rac1 inhibitor that has been recently become available (see Materials and Methods). This compound prevented in a dose-dependent manner both the cytotoxicity and the activation of JNK by Aplidin® in MDA-MB-231 (Figure 8a) and HeLa (Figure 8b) cells. Together with the siRNA data, these results show the importance of Rac1 activation for Aplidin® action.

In addition, we studied MKP-1, a dual phosphatase that dephosphorylates and deactivates members of the MAPK family (JNK and p38 with preference over ERK), and is regulated by multiple pathways and agents.[27] By Western blotting we found that Aplidin® decreased the levels of MKP-1
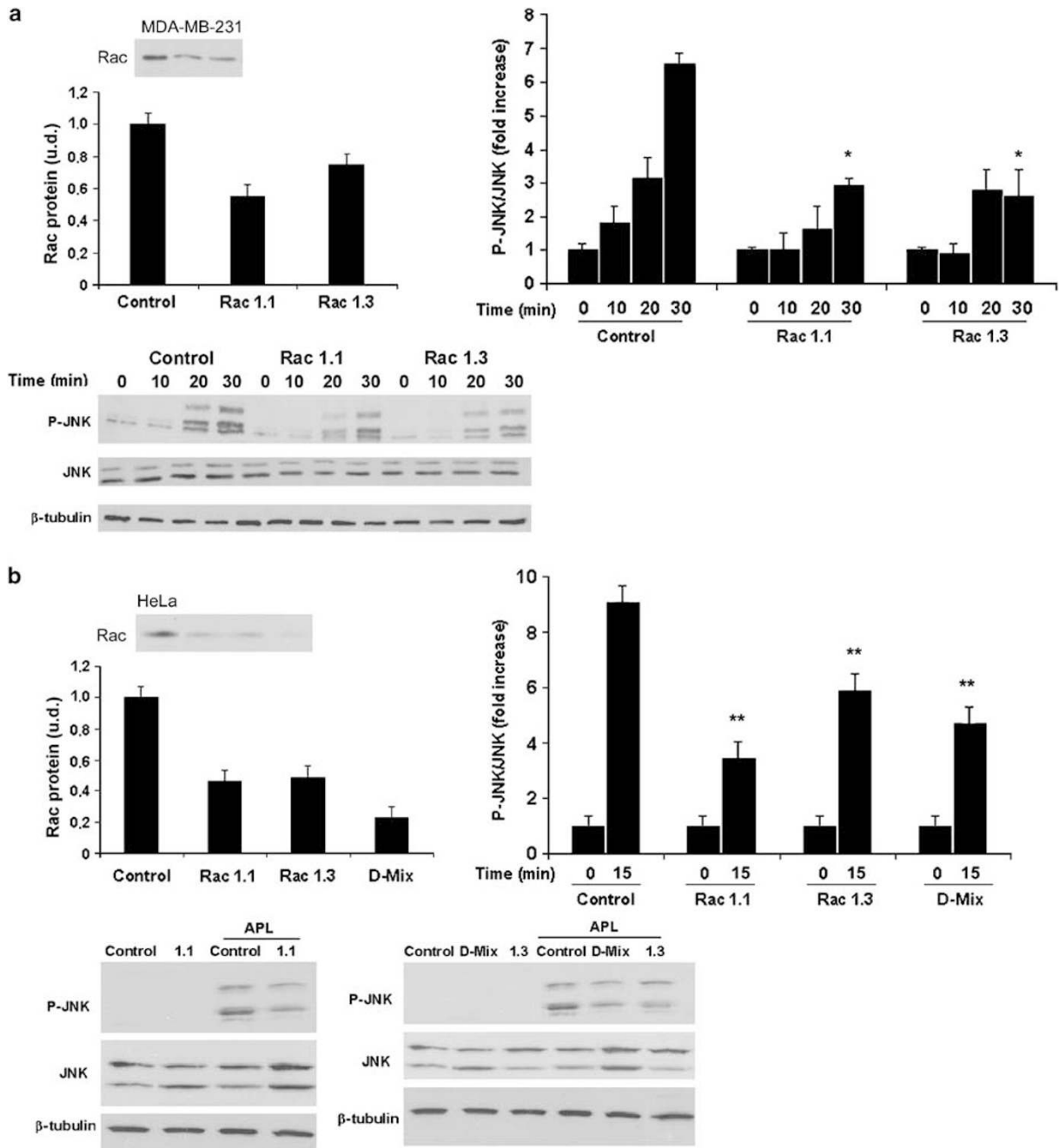
Figure 7 Downregulation of Rac1 inhibits JNK activation by Aplidin®. MDA-MB-231 (**a**) and HeLa (**b**) cells were transfected as described in Materials and methods with control or specific Rac1 siRNA oligonucleotides (Rac 1.1, Rac 1.3, D-Mix). After 16 h cells were treated or not with Aplidin® (500 nM) and incubated for the indicated times before cell extracts were prepared for analysis of Rac activity and Western blotting of Rac1, total- and phospho-JNK and β-tubulin protein levels as described before. Graphics show mean values and standard deviation corresponding to three independent experiments. *$P < 0.05$; **$P < 0.001$. Results from a representative experiment obtained in each cell line are shown in the lower part of (**a**) and (**b**)

(Figure 9a). This effect does not depend on protein synthesis *de novo* as it was not prevented by the translation inhibitor cycloheximide (data not shown). As expected, overexpression of exogenous MKP-1 inhibited JNK activation by Aplidin® in MDA-MB-231 cells (Figure 9b). Lactacystin, an irreversible proteasome inhibitor, consistently caused partial rescue of MKP-1 downregulation, indicating that the effect of Aplidin® is partly due to the modulation of MKP-1 protein stability at the proteasome level (Figure 9c). In contrast to Rac1 activation, exogenous GSH did not prevent the reduction of MKP-1 levels (data not shown). MKP-1 downregulation does not reflect an unspecific effect on cellular phosphatases, as Aplidin®-treated cells showed no changes in the total cellular phosphatase activity, as measured by the *p*-nitrophenyl phosphate method (data not shown), although effects on phosphatases other than MKP-1 cannot be ruled out. The

Table 4 Effect of Rac 1.1 downregulation on Aplidin®-induced apoptosis

Cell line	Living cells		Early apoptotic		Late apoptotic	
	% Cells	% Control	% Cells	% Control	% Cells	% Control
HeLa						
siControl	60.4±3	100	1.5±0	100	11.0±2	100
siControl+APL	17.8±1	29	1.8±0	120	35.8±3	325
siRac	54.3±4	100	2.4±0	100	14.8±1	100
siRac+APL	32.6±2	60	1.5±0	44	31.2±3	209
MDA-MB-231						
siControl	60.4±6	100	2.4±0	100	16.2±3	100
siControl+APL	42.3±1	70	4.0±0	167	25.4±2	157
siRac	60 9±6	100	1.7±0	100	15.6±3	100
siRac+APL	59.0±5	97	1.9±0	112	17.8±1	114

Cells were co-transfected with Rac 1.1 or control siRNA together with a FAM-labeled unrelated siRNA. Seven hours after transfection cells were exposed to 500 nM Aplidin (APL) or left untreated for additional 24 h. FITC-Annexin V (AV) and propidium iodide (PI) staining was then estimated by flow cytometry. *Living cells* refer to PI−/AV−, *early apoptotic* to PI−/AV+ and *late apoptotic* to PI+/AV+. Results are shown as percentages of the transfected population (% *cells*) and of the corresponding untreated control (% *control*). Mean values obtained in two independent experiments performed in duplicate are shown. Percentages left correspond to necrotic cells and cell debris
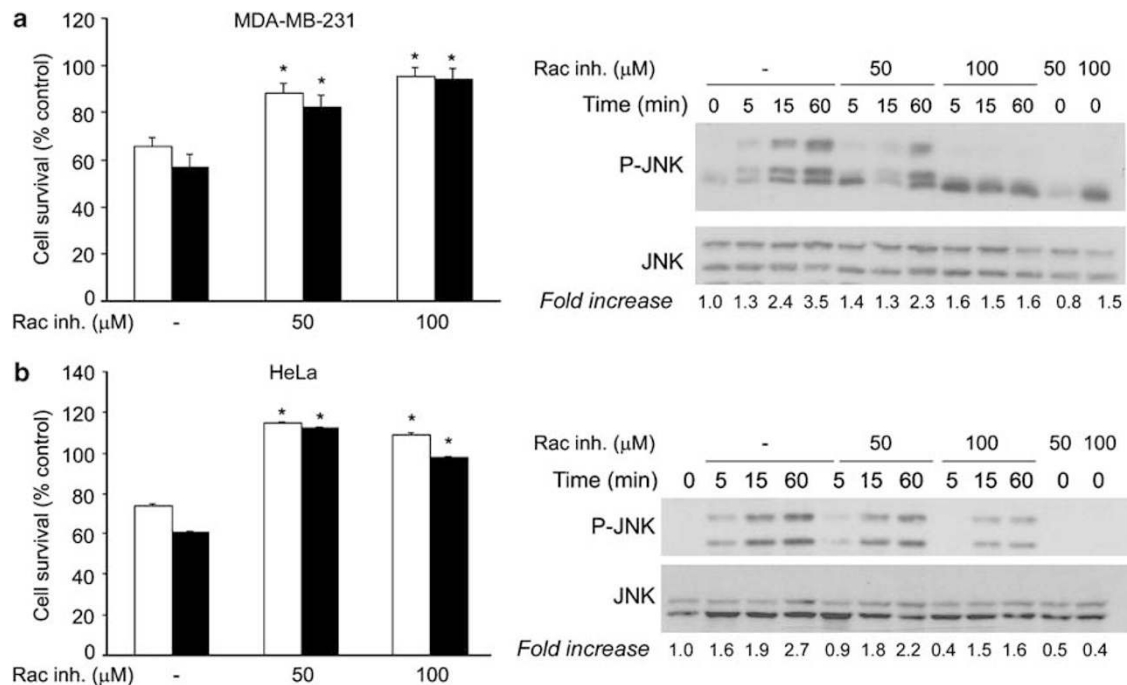
Figure 8 Rac1 inhibitor prevents Aplidin®-induced cytotoxicity and JNK activation. (**a**) Effect of Rac1 inhibitor on Aplidin®-induced cytotoxicity (left part) measured by the MTT method. MDA-MB-231 cells were pretreated overnight with the indicated doses of Rac1 inhibitor and then for a further 24 h with 150 nM (white columns) or 500 nM (black columns) of Aplidin®. The Rac1 inhibitor was kept in the medium until the end of the experiment. Three experiments were performed in triplicate. *$P < 0.05$. Effect of overnight pretreatment with Rac1 inhibitor on the activation of JNK by Aplidin® (right part). Results from one of the three experiments using the indicated doses and time points are shown. (**b**) Same as in (**a**) using HeLa cells

importance of MKP-1 downregulation for Aplidin® action was investigated by studying the sensitivity to the drug of cells lacking the *mkp-1* gene. MEF *mkp-1*$^{-/-}$ showed slightly higher sensitivity to MEF wild-type, particularly at low drug concentrations (Figure 9d). This is consistent with the higher level of JNK activation induced by the drug in MEF *mkp-1*$^{-/-}$ cells (Figure 9e).

As the effects of Aplidin® on Rac1 and MKP-1 are rapid and post-transcriptional, we assessed whether gene expression is required for its cytotoxicity. To this end, MDA-MB-231 and

MCF-7 cells were pre-incubated for 30 min with actinomycin D (transcription inhibitor) or cycloheximide (translation inhibitor) and then with Aplidin® for 4 or 7 h. The culture medium was then changed and cells were extensively washed and incubated in fresh medium. No differences in cell viability 48 h after drug addition were found in the presence or absence of the inhibitors, indicating that Aplidin® cytotoxicity does not require gene expression *de novo* (data not shown) in spite of the fact that p65/*REL*A and several genes of the *JUN* and *FOS* families are activated.[10]
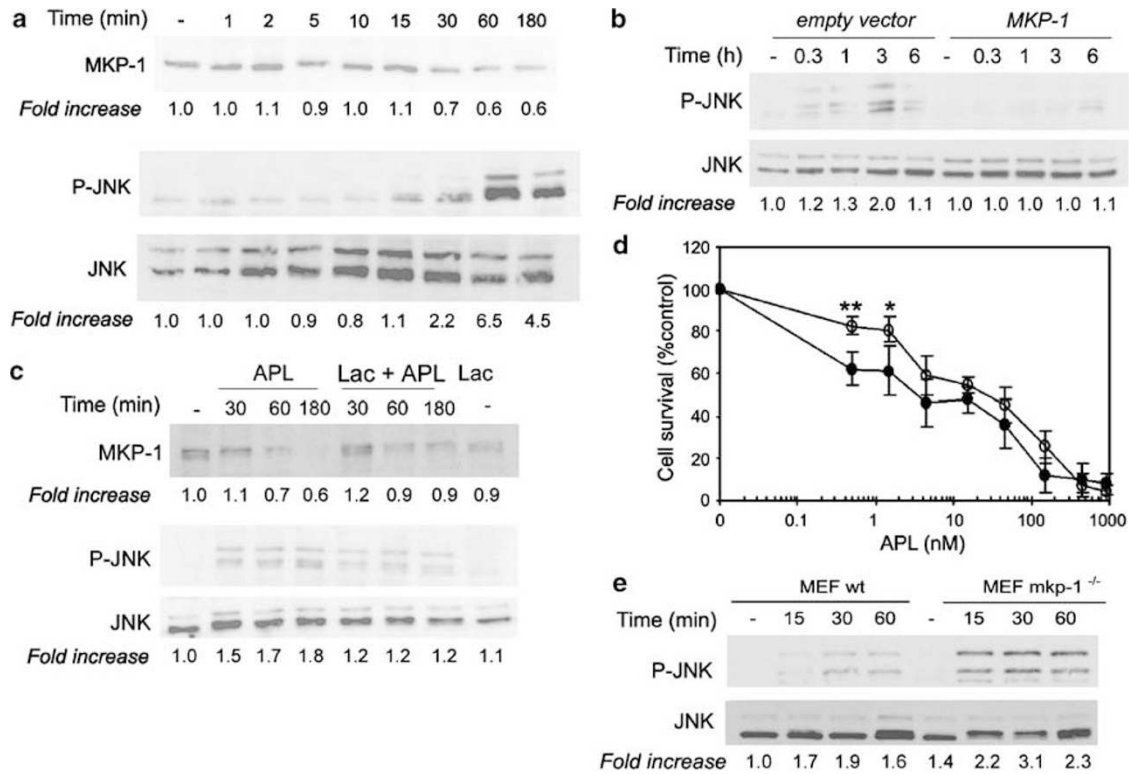
Figure 9 Aplidin® downregulates MKP-1 protein. (**a**) Levels of MKP-1 protein (upper part), activated JNK (middle part) and total JNK (lower part) in cells treated with 500 nM Aplidin® for the indicated times as measured by Western blot. Changes in the amount of MKP-1 and phospho-JNK (normalized to that of total JNK) are shown. (**b**) Effect of MKP-1 overexpression on the activation of JNK by Aplidin®. MDA-MB-231 cells were stably transfected with either an empty vector of a MKP-1 expression vector. MKP-1 protein levels were estimated as in (**a**). (**c**) Effect of lactacystin on the downregulation of MKP-1 protein by Aplidin®. Cells were pretreated with lactacystin (1 μM) for 3 h before Aplidin® addition (time 0), and the levels of MKP-1 protein were estimated Western blotting at the indicated times. In all cases (**a–d**), bands from a representative experiment and mean values obtained in three experiments are shown. (**d**) Analysis of the effect of 48 h treatment with the indicated doses of Aplidin® on the survival of MEF wild-type (open circles) and *mkp-1*$^{-/-}$ (solid circles) measured by the MTT method. *$P<0.1$; **$P<0.05$. (**e**) Analysis by Western blotting of the levels of phosphorylated and total JNK in MEF wild-type and *mkp-1*$^{-/-}$ treated with 500 nM Aplidin®. Values of JNK activation were normalized to those of total JNK protein and shown as fold-increase with respect to untreated wild-type cells

Discussion

We have examined the mechanism of the pro-apoptotic action of the marine antitumor agent Aplidin® in human MDA-MB-231 breast cancer cells. Aplidin® rapidly induces cell death at doses in the nanomolar range.[4] This potent activity highlights the need to identify the precise action of the drug at the molecular level in order to search for target-directed screening methods, to improve its activity by rational modelling of the molecule, to analyze the activity of derivatives, and to design combined treatments with other antitumor drugs.

In this study we show that Aplidin® disrupts cellular glutathione homeostasis (GSSG/GSH ratio) by causing GSH depletion by several mechanisms including alteration of GPx and GR activity, and GSH extrusion to the medium. In addition, S-glutathiolation of proteins cannot be ruled out. Glutathione homeostasis is strictly regulated as a protection against oxidative stress. Aplidin® induces cellular oxidative stress as shown by the generation of ROS, which is reflected in the increase of lipids and DNA oxidation. Reactive oxygen species production is expected to deplete cellular antioxidant defenses, which enhances oxidative stress and cell injury. Our data indicate that Aplidin® induces GSH depletion, which in turn causes ROS production, as compounds that regulate GSH levels (Ebselen, N-acetylcystheine) inhibit Aplidin® action, while a range of general antioxidants do not.

Upon oxidative stress GSSG may exit from the cells,[28] but GSH extrusion through specific carriers is more important as an early step in the commitment of cells to apoptosis, being the cause rather than the consequence of oxidative stress by altering the reducing power of cells.[29,30] Thus, human monocytic U937 and hepatoma HepG2 cells extrude GSH concomitantly to or before the development of apoptosis induced by puromycin or etoposide, a process that is ameliorated by methionine or cystathionine, inhibitors of the sinusoidal GSH transport system.[30] Likewise, apoptosis of Jurkat T lymphocytes caused by anti-Fas/Fas ligation induces a rapid efflux of GSH.[31] Our data using GSH transport inhibitors and direct measurement in the medium indicate that GSH extrusion is involved at least in late stages of Aplidin® action.

There is rapid exchange between mitochondrial and cytosolic GSH levels, and administration of GSH esters increases GSH levels in mitochondria more than those in the cytosol.[32] The finding that exogenously added GSH prevented the loss of mitochondrial membrane potential caused by Aplidin® strongly supports a critical role of GSH depletion in its cytotoxic action. Together, our results suggest that

Aplidin® primarily and specifically induces GSH depletion, which may then cause oxidative stress affecting cellular macromolecules such as membrane phospholipids and DNA.

Previous data showed that sustained JNK activation is critical for Aplidin®-induced apoptosis.[10] Many regulators of JNK are known.[33] Among them, Rac acts upstream of kinase cascades that activate JNK via dual phosphorylation in threonine (Thr) and tyrosine (Tyr) residues within a Thr-Pro-Tyr motif in the activation loop.[34] MKP-1 phosphatase inhibits JNK activity by dephosphorylation of these two residues. In addition, activated Rac induces ROS production through a direct effect on the mitochondria in rabbit synovial fibroblasts.[35] Our results reveal two rapid, gene expression-independent mechanisms by which Aplidin® activates JNK: the combination of initial Rac1 activation and later MKP-1 downregulation is expected to lead to rapid, strong and sustained activation of JNK. The effect of Rac1, but not MKP-1, depends on GSH depletion. Our results showing that Rac1 downregulation by using siRNA reduces JNK activation and cytotoxicity by the drug indicate the importance of Rac1 activation for Aplidin® action. The reported finding that Rac1-deficient cells are not viable shows that a certain level of Rac1 is required for cell survival. This may explain the inability of Rac1 siRNA to completely abolish Rac1 expression and JNK activity in drug-treated cells. Further support for the crucial role of Rac1 in Aplidin® action derives from the reduction of drug-induced JNK activation and cytotoxicity. Taken together our data demonstrate that Aplidin® causes Rac1 activation leading to JNK activation and the induction of apoptosis in two different cell types.

The finding that MKP-1 deficient cells are only slightly more sensitive to the drug does not rule out a role of JNK in Aplidin®-induced cytotoxicity, since the activation of JNK in these cells is also slightly higher than in wild-type cells, probably due to compensatory mechanisms involving other phosphatases. Supporting a role of MKP-1 downregulation in apoptosis, it has been reported that MKP-1 stabilization by proteasome inhibitors is anti-apoptotic through the inhibition of JNK,[36] and chondrocyte death by tumor necrosis factor-α (TNF-α) is associated with sustained JNK activation, probably due to MKP-1 downregulation.[37] Presumably, MKP-1 downregulation potentiates JNK activation induced by Aplidin® via Rac1 activation (which is more evident at low doses) similarly to what happens in renal cancer cells, in which the MKP-1 expression inhibitor Ro-318220 enhances the pro-apoptotic effect of the JNK activator anisomycin.[38] There are many phosphatases acting on JNK;[34] however, MKP1 and MKP2 appear relevant as they are overexpressed in human breast cancer, and thus responsible for reduced JNK activity.[39] MKPs may thus be viable targets for therapeutic intervention to enable expression of the pro-apoptotic activity of JNK in breast cancer,[39] and Aplidin® may thus be a valuable therapeutic tool.

The mechanism of Aplidin®-induced apoptosis resembles several pathological cell death processes. One of them is the toxic effect of the combination of high homocysteine levels and Cu^{2+}. This combination decreases the GSH content, triggers the generation of ROS and induces loss of mitochondrial membrane potential and caspase-dependent apoptosis in vascular cells.[40] These data indicate similarities between Aplidin® and homocysteine/Cu^{2+} in the control of cellular GSH content. Additionally, the mechanism of action of Aplidin® is similar, but not identical to that of glutamate in neurons. Exogenous glutamate inhibits cystine uptake through the cystine/glutamate antiporter leading to GSH depletion, lipoxygenase activation, ROS production, opening of cGMP-gated channels and influx of extracellular Ca^{2+}, a form of cell death with characteristics of apoptosis and necrosis known as oxytosis.[41] In contrast to Aplidin®, this process is inhibited by protein kinase C activation, and involves damage of mitochondria and other organules but not DNA fragmentation. Glutamate toxicity in the mouse HT22 neuronal cell line causes two waves of ROS, an early one linked to GSH depletion, followed by a greater wave dependent on the influx of extracellular Ca^{2+}.[42] Together, these studies show that multiple agents can induce GSH depletion via different mechanisms (extrusion, inhibition of glutathione peroxidase, cystine antiporter, γ-glutamylcysteine synthetase or γ-glutamyl transpeptidase), and that GSH depletion can trigger distinct pathways leading to different forms of cell death depending on the strength of the stimulus and cellular ATP content.

Our results show that Aplidin® has a complex mechanism of cytotoxicity, which has similarities but also differences with other physiological and pathological cell death processes. The induction of GSH depletion is pivotal for downstream events of apoptosis: it triggers Rac1 activation, which together with MKP-1 downregulation leads to sustained JNK activation and cell death. Ongoing efforts seek to identify the primary cellular target(s) of Aplidin® responsible for the disruption of GSH homeostasis and Rac1 activation, and of MKP-1 downregulation. The strong pro-apoptotic activity and promising clinical data of Aplidin® emphasize the interest of this study.

Materials and Methods

Cell lines, antibodies, and reagents

MDA-MB-231 (obtained from the American Type Culture Collection, Rockville, USA), HeLa and LS174-T cells were grown in Dulbecco's modified Eagles' medium (DMEM) supplemented with 10% FCS and 1 mM glutamine (all from GIBCO-Invitrogen, Paisley, UK). Mouse embryo fibroblasts deficient for GSTπ1π2 (MEF GSTπ1π2$^{-/-}$) or for JNK (jnk1/2$^{-/-}$) were donated by Drs. KD Tew/L Gate (Fox Chase Cancer Center, Philadelphia) and Dr. E Wagner (Institut für Molekulare Pathologie, Vienna), respectively, and grown in the same medium. To reduce Cu^{2+} levels in the culture medium (DMEM plus 10% FCS) we used Chelex 100 resin (Bio-Rad, Hercules, CA, USA) following the manufacturer's recommendations. Aplidin® is manufactured by Pharma Mar S.A. (Madrid, Spain). Stock solutions were freshly prepared in dimethylsulfoxide (DMSO) and diluted in the cell culture to final concentrations as indicated. Ascorbic acid, diphenelene iodonium (DPI), Tiron, catalase, glutathione reduced ethyl ester (GSH), N-acetylcysteine (NAC), Ebselen (EBS), L-buthionine,S,R-sulfoximine (BSO), cupric sulfate ($Cu2^+$), bromosulfophthalein (BSP), butylated hydroxyanisole (BHA), bathocuproinedisulfonic acid (BCPS), lactacystin, and ATK (Arachidonyl-L-trifluoromethylketone) were from Sigma Chemical Co. (St. Louis, MO, USA); baicalein, 5,6-dehydro-arachidonic acid; 12-nordihydroguaiaretic acid were from Cayman; RHC-80267/U-57908 from Biomol; and 5-bromo-

chloro-3-indolyl phosphate/nitroblue tetrazolium (BCIP/NBT) and Rac1 inhibitor (NSC23766) were from Calbiochem.

Antibodies used were anti-JNK1 and anti-MKP1 were from Santa Cruz; anti-phospho-JNK1 from New England Biolabs/Cell Signaling; anti-GST$\pi1\pi2$ from Calbiochem; anti-HA from Babco; anti-phosphotyrosine and anti-Rac1 monoclonal antibodies were from Transduction Laboratories/BD Biosciences (Heidelberg, Germany).

Animals

C57/Bl6 (mkp-1 +/−; +/+) blastocysts generated by the Rodrigo Bravo laboratory at Bristol–Myers Squibb Pharmaceutical Research Institute[43] were supplied by the Jackson laboratory and subsequently bred in house. All experiments were performed according to European Union and German statutory regulations. The genotype of the mice was established by tissue biopsies and subsequent DNA analysis by PCR using two separate reactions with the primer pair 5′-CAGG TACTGTGTGTCGGTGGTGCTAATG-3′ and 5′-CTATATCCTCCTGGCA CAATCCTCCTAG-3′ for the wild-type allele or 5′-AAATGTGTCAGTTT CATAGCCTGAAGAACG-3′ and 5′-CTATATCCTCCTGGCACAATCC TCCTAG-3′ for the mutant allele.

Preparation of mouse embryonic fibroblasts

The primary wild-type and MKP-1-deficient (mkp-1$^{-/-}$) MEF were isolated from 15 to 16-day-old embryos. Head and internal organs of the embryos were removed on a Petri plate with PBS and the trunk was dissected in 10 ml DMEM supplemented with 0.05% trypsin (Invitrogen) with fine scissors. After incubation at 37°C for 10 min, the solution was pipetted up and down five times with a 20 ml glass pipette. This was repeated with 10 ml and 5 ml glass pipettes with 10 min incubation at 37°C in between. Once complete, trypsinization was terminated by adding 5 ml fetal calf serum (FCS). Cell suspension and clumps were transferred into a Falcon tube and incubated for 2 min at 4°C to sediment the clumps. Approximately 10 ml of the supernatant was transferred into a new tube through a 70 μm cell strainer (Falcon) leaving clumps behind. After centrifugation at 2000 r.p.m. for 5 min at room temperature, the pellet was washed once in 10 ml complete medium (DMEM supplemented with 10% FCS and 100 U/ml penicillin, 100 μg/ml streptomycin; Invitrogen). Cells were counted and plated up to 10×10^6 cells per 15 cm plate. The next day, the medium was changed and the cells were cultured until they reached confluence. The cells were subcultured at a density of $5–10 \times 10^6$ cells per 15 cm plate every 3 days. This process was repeated until they reached crisis and became established cell lines.

Flow cytometry analyses

Apoptotic cells were determined by their hypochromic, subdiploid staining profiles (subG1 population). Cells treated or not with Aplidin® were stained with PI and analyzed by flow cytometry (FACScan, Becton Dickinson, San Jose, CA, USA, equipped with a 488 nm argon ion laser). For staining, one million cells were harvested, washed in PBS and then fixed with 70% ethanol. Fixed cells were treated with DNAse-free RNAse for 30 min at 37°C, washed in PBS, centrifuged, and incubated in PBS-containing PI (25 μg/ml; Sigma). Forward light scatter characteristics were used to exclude the cell debris from the analysis. Ten thousand events per sample were acquired for data analysis using CELLQUEST software by selective gating to exclude doublet cells. The results of the DNA content were modeled using ModFit (VERITY Software House, Inc., Topsham, ME). In RNA interference studies, FITC-annexin V and PI staining were analyzed: non-apoptotic living cells were FITC-annexin-V negative/PI negative, early apoptotic cells were FITC-annexin-V positive/PI negative, and late apoptotic cells were FITC-annexin-V positive/PI positive, whereas necrotic cells were FITC-annexin-V negative/low-PI positive.

To measure mitochondrial membrane potential ($\Delta\Psi m$), mitochondria were selectively probed with potential-sensitive JC-1 (5,5′,6,6′-tetra-chloro-1,1′,3,3′-tetraethyl-benzimidazolylcarbocyanine iodide) (Molecular Probes). JC-1 was stocked as 1 mg/ml in DMSO and freshly diluted with complete culture medium. After treatments cells were harvested and incubated with medium containing JC-1 (10 μg/ml) for 10 min. Finally, cells were washed and resuspended in 1 ml PBS for flow cytometry analysis. JC-1 exhibits $\Delta\Psi m$-dependent accumulation in mitochondria, indicated by a shift in its fluorescence emission from green to red due to the formation of J-aggregates. Mitochondrial depolarization is thus indicated by a decrease in the red/green fluorescence ratio.

To analyze ROS, cells were stained with 2′,7′-dichlorofluorescein diacetate (2′,7′-DCFH-DA) (Molecular Probes). After incubation, the cells were trypsinized, washed in cold PBS and incubated for 30 min at 37°C in medium containing 2 μM 2′,7′-DCFH-DA and 5 μg/ml PI. To ensure that only living cells were analyzed, those that incorporated PI were excluded. The fluorescence intensity of intracellular 2′,7′-DCFH-DA was determined in living cells by the CELLQUEST software.

Intracellular Ca^{2+} levels were estimated by labeling the cells with 1 μM Fluo-4 (Molecular Probes). Plasma membrane permeability was measured by labeling cells with 1 μg/ml Fluorescein diacetate (FDA; Molecular Probes) and 5 μg/ml PI for 30 min at 37°C in normal growth medium.

Immunoprecipitation and Western-blot analysis

To study the effect of Aplidin® on the activity of JNK cells were preincubated for 24 h in serum-free medium. For immunoprecipitation cells were lysed in modified RIPA buffer (50 mM Hepes pH 7.4, 150 mM NaCl, 10% glycerol, 1.5 mM MgCl2, 1 mM EGTA, 1% Triton X-100, 1% deoxycholic acid, 0.1% SDS, 1 mM Na3VO4, 25 mM β-glycerolphosphate, 100 mM NaF, 10 μg/ml leupeptin, 10 μg/ml aprotinin, 1 mM PMSF). Lysates were precleared by incubation with protein G-Sepharose at 4°C for 30 min and then incubated overnight with the corresponding antibody (1 μg/ml). After 1 h incubation with protein G-sepharose, immune complexes were washed three times in the same RIPA buffer lacking deoxycholic acid and SDS and then three times with HNTG (50 mM Hepes pH 7.4, 150 mM NaCl, 10% glycerol, 0.1% Triton X-100, 1 mM Na3VO4, 10 μg/ml leupeptin, 10 μg/ml aprotinin, 1 mM PMSF) and electrophoresed in 10% acrylamide gels. For Western-blot analysis cell protein extracts were prepared as described.[4] Protein extracts were electrophoresed in 8 or 12% polyacrylamide gels and transferred to nitrocellulose (Immobilon P, Millipore) membranes. The filters were washed, blocked with 5% BSA in Tris-buffered saline (TBS) (25 mM Tris pH 7.4, 136 mM NaCl, 2.6 mM KCl, 0.5% Tween-20), and incubated overnight at 4°C with the appropriate antibody. Blots were washed three times for 10 min in PBS + 0.1% Tween-20 and incubated with HRP- or alkaline phosphatase-conjugated secondary antibodies for 1 h at room temperature. Blots were developed by a peroxidase reaction using the ECL detection system (G.E. Health Care) or the BCIP/NBT reaction and a colorimetric assay.

Cell transfections

Cells were transfected at around 50% confluence in 6-cm dishes with 5 μg of DNA using Lipofectamine (Invitrogen). We used 3 μg of expression plasmids for mouse MKP-1 (donated by Dr. P Muñoz, Barcelona) or

thioredoxin (donated by Dr. J Yodoi, Kyoto) and the pSG5 vector as carrier to adjust the total amount of DNA. After overnight incubation with Lipofectamine-DNA mixtures, transfected cells were washed twice in PBS and incubated with fresh medium supplemented with 0.5% FCS. Each treatment was carried out in triplicate cultures. Protein extracts were prepared following standard procedures and analyzed by Western blotting.[4]

Determination of oxidative stress-related parameters

Lipid peroxidation assays: Malondialdehyde (MDA) was measured by High-pressure liquid chromatography (HPLC) as described.[44] DNA oxidation measurement: cell DNA was isolated and digested as described.[45] Levels of 8-oxo-2′-deoxyguanosine (8-oxo-dG) were measured by HPLC (Waters ODS HPLC column) followed by electrochemical and ultraviolet absorbance detection as described.[45] Cellular content of GSH and GSSG were measured by HPLC as previously described.[46,47]

Determination of GSH in the extracellular medium

The content of GSH was quantified by the fluorometric assay of Hissin and Hilf.[48] The method takes advantage of the reaction of reduced glutathione with o-phthalaldehyde (OPT) at pH 8.0. Conditioned culture medium was centrifuged to eliminate cells and debris and 50 μl was placed in a 96-well multiwell plus15 μl of 1 M NaOH and 175 μl of 0.1 M sodium phosphate buffer pH 8.0, containing 5 mM EDTA. Finally, 10 μl per well of a stock solution of OPT (10 mg/ml) in methanol was added and after 15 min at room temperature in the dark, fluorescence was measured at an emission wavelength of 460 nm and an excitation wavelength of 340 nm. The results of the samples were referred to those of a standard curve of GSH (5 ng – 1 μg).

Measurement of glutathione peroxidase (GPx) and reductase (GR) activity

The activity of these two enzymes in extracts from cells treated or not with Aplidin® was measured using commercial kits following the manufacturer's recommendations (Cayman).

Cell survival – MTT assays

[3-(4,5-dimethythiazol-2-yl)-2,5-diphenyl] tetrazolium bromide (MTT) assays were performed following the manufacturer's instructions (MTT cell proliferation Kit I, Roche Diagnostics, Mannheim, Germany).

Rac1 activity assays

Bacterial expression of fusion proteins. The plasmid pGEX-PAK-CRIB containing the Rac1-binding domain fused to GST was kindly provided by JG Collard (The Netherlands Cancer Institute). GST-fusion protein was purified (from *Escherichia coli* BL21 (DE3) harboring these plasmids) following the method previously described.[49] For *in vitro* binding assays, mammalian cells were lysed in cold lysis buffer and nucleus-free supernatants were incubated with the GST-fusion protein on glutathione-Sepharose beads and analyzed as previously described.[49]

RNA interference

siRNA duplexes specific for Rac1 (Rac1.1, bases 529–550; Rac1.3, bases 605–626) were designed as described.[50] The siRNA sequence sense strand used as negative control for siRNA activity was AUUGUAUGC GAUCGCAGACdTdT. Control and Rac1 siRNA duplexes were purchased from Ambion (Austin, TX, USA). In addition, we also used the SMARTpool® siRNA reagent M-003560-02-0020 for human RAC1 (D-Mix) purchased from Dharmacon. siRNA duplexes (40 nM) were transfected using X-tremeGENE siRNA transfection reagent (Roche) and transfectants assayed 24 h post-transfection. Transfections did not affect cell viability.

To analyze the effect of Rac1 siRNA by flow cytometry cells were co-transfected with Rac1.1 or Control siRNA (40 nM) and 5′-carboxy-fluorescein (FAM)-labeled unrelated negative control siRNA (4 nM). In addition, parallel cultures were transfected with β-actin siRNA instead of Rac1.1. All these siRNA oligonucleotides were from Ambion.

References

1. Sakai R, Rinehart KL, Kishore V, Kundu B, Faircloth G, Gloer JB, Carney JR, Namikoshi M, Sun F, Hughes Jr RG, García Grávalos D, de Quesada TG, Wilson GR and Heid RM (1996) Structure–activity relationships of the didemnins. J. Med. Chem. 39: 2819–2834.
2. Lobo C, García-Pozo SG, Nuñez de Castro I and Alonso FJ (1997) Effect of dehydrodidemnin B on human colon carcinoma cell lines. Anticancer Res. 17: 333–336.
3. Depenbrock H, Peter R, Faircloth GT, Manzanares I, Jimeno J and Hanauske AR (1998) In vitro activity of aplidine, a new marine-derived anti-cancer compound, on freshly explanted clonogenic human tumour cells and haematopoietic precursor cells. Br. J. Cancer 78: 739–744.
4. Cuadrado A, García-Fernández LF, González L, Suárez Y, Losada A, Alcaide V, Martínez T, Fernández-Sousa JM, Sánchez-Puelles JM and Muñoz A (2003) Aplidin induces apoptosis in human cancer cells via glutathione depletion and sustained activation of the epidermal growth factor receptor, Src, JNK, and p38 MAPK. J. Biol. Chem. 278: 241–250.
5. Faircloth G, Hanauske A, Depenbrock H, Peter R, Crews C, Manzanares I, Meely K, Grant W and Jimeno J (1997) Preclinical characterization of Aplidine (APD), a new marine anticancer depsipeptide (MADEP). Proc. Am. Assoc. Cancer Res. 103.
6. Erba E, Bassano L, Di Liberti G, Muradore I, Chiorino G, Ubezio P, Vignati S, Codegoni A, Desiderio MA, Faircloth G, Jimeno J and D'Incalci M (2002) Cell cycle phase perturbations and apoptosis in tumour cells induced by aplidine. Br. J. Cancer 86: 1510–1517.
7. Erba E, Ronzoni S, Bergamaschi D, Bassano L, Desiderio AM, Faircloth GT, Jimeno J and D'Incalci M (1999) Mechanism of antileukemic activity of Aplidine. Proc. Am. Assoc. Cancer Res. 3.
8. Yao L (2003) Aplidin PharmaMar. IDrugs 6: 246–250.
9. García-Fernández LF, Losada A, Alcaide V, Alvarez AM, Cuadrado A, González L, Nakayama K, Nakayama KI, Fernández-Sousa JM, Muñoz A and Sánchez-Puelles JM (2002) Aplidin induces the mitochondrial apoptotic pathway via oxidative stress-mediated JNK and p38 activation and protein kinase C delta. Oncogene 21: 7533–7544.
10. Cuadrado A, González L, Suárez Y, Martínez T and Muñoz A (2004) JNK activation is critical for Aplidin-induced apoptosis. Oncogene 23: 4673–4680.
11. Gajate C, An F and Mollinedo F (2003) Rapid and selective apoptosis in human leukemic cells induced by Aplidine through a Fas/CD95- and mitochondrial-mediated mechanism. Clin. Cancer Res. 9: 1535–1545.

12. Broggini M, Marchini SV, Galliera E, Borsotti P, Taraboletti G, Erba E, Sironi M, Jimeno J, Faircloth GT, Giavazzi R and D'Incalci M (2003) Aplidine, a new anticancer agent of marine origin, inhibits vascular endothelial growth factor (VEGF) secretion and blocks VEGF-VEGFR-1 (flt-1) autocrine loop in human leukemia cells MOLT-4. Leukemia 17: 52–59.

13. Taraboletti G, Poli M, Dossi R, Manenti L, Borsotti P, Faircloth GT, Broggini M, D'Incalci M, Ribatti D and Giavazzi R (2004) Antiangiogenic activity of aplidine, a new agent of marine origin. Br. J. Cancer 90: 2418–2424.

14. Erba E, Serafini M, Gaipa G, Tognon G, Marchini S, Celli N, Rotilio D, Broggini M, Jimeno J, Faircloth GT, Biondi A and D'Incalci M (2003) Effect of Aplidin in acute lymphoblastic leukaemia cells. Br. J. Cancer 89: 763–773.

15. Macho A, Hirsch T, Marzo I, Marchetti P, Dallaporta B, Susin SA, Zamzami N and Kroemer G (1997) Glutathione depletion is an early and calcium elevation is a late event of thymocyte apoptosis. J. Immunol. 158: 4612–4619.

16. White AR and Cappai R (2003) Neurotoxicity from glutathione depletion is dependent on extracellular tRac1e copper. J. Neurosci. Res. 71: 889–897.

17. Kramer BC, Yabut JA, Cheong J, Jnobaptiste R, Robakis T, Olanow CW and Mytilineou C (2004) Toxicity of glutathione depletion in mesencephalic cultures: a role for arachidonic acid and its lipoxygenase metabolites. Eur. J. Neurosci. 19: 280–286.

18. Shornick LP and Holtzman MJ (1993) A cryptic, microsomal-type arachidonate 12-lipoxygenase is tonically inactivated by oxidation-reduction conditions in cultured epithelial cells. J. Biol. Chem. 268: 371–376.

19. Adler V, Yin Z, Fuchs SY, Benezra M, Rosario L, Tew KD, Pincus MR, Sardana M, Henderson CJ, Wolf CR, Davis RJ and Ronai Z (1999) Regulation of JNK signaling by GSTp. EMBO J. 18: 1321–1334.

20. Lo YY, Wong JM and Cruz TF (1996) Reactive oxygen species mediate cytokine activation of c-Jun NH2-terminal kinases. J. Biol. Chem. 271: 15703–15707.

21. Seimiya H, Mashima T, Toho M and Tsuruo T (1997) c-Jun NH2-terminal kinase-mediated activation of interleukin-1beta converting enzyme/CED-3-like protease during anticancer drug-induced apoptosis. J. Biol. Chem. 272: 4631–4636.

22. Srivastava RK, Mi QS, Hardwick JM and Longo DL (1999) Deletion of the loop region of Bcl-2 completely blocks paclitaxel-induced apoptosis. Proc. Natl. Acad. Sci. USA 96: 3775–3780.

23. Chen K, Vita JA, Berk BC and Keaney Jr JF (2001) c-Jun N-terminal kinase activation by hydrogen peroxide in endothelial cells involves SRC-dependent epidermal growth factor receptor transactivation. J. Biol. Chem. 276: 16045–16050.

24. Coso OA, Chiariello M, Yu JC, Teramoto H, Crespo P, Xu N, Miki T and Gutkind JS (1995) The small GTP-binding proteins Rac11 and Cdc42 regulate the activity of the JNK/SAPK signaling pathway. Cell 81: 1137–1146.

25. Minden A, Lin A, Claret FX, Abo A and Karin M (1995) Selective activation of the JNK signaling cascade and c-Jun transcriptional activity by the small GTPases Rac1 and Cdc42Hs. Cell 81: 1147–1157.

26. Alberts AS and Treisman R (1998) Activation of RhoA and SAPK/JNK signalling pathways by the RhoA-specific exchange factor mNET1. EMBO J. 17: 4075–4085.

27. Kelly K and Chu Y (2000) The regulation of MAP kinase pathways by MAP kinase phosphatases. In Signaling networks and cell cycle control: The molecular basis of cancer and other diseases, Gutkin JS (ed) (Totowa, NJ, USA: Humana Press Inc.) pp. 165–182.

28. Reed DJ (1990) Glutathione: toxicological implications. Annu. Rev. Pharmacol. Toxicol. 30: 603–631.

29. Ghibelli L, Coppola S, Rotilio G, Lafavia E, Maresca V and Ciriolo MR (1995) Non-oxidative loss of glutathione in apoptosis via GSH extrusion. Biochem. Biophys. Res. Commun. 216: 313–320.

30. Ghibelli L, Fanelli C, Rotilio G, Lafavia E, Coppola S, Colussi C, Civitareale P and Ciriolo MR (1998) Rescue of cells from apoptosis by inhibition of active GSH extrusion. Faseb J. 12: 479–486.

31. van den Dobbelsteen DJ, Nobel CS, Schlegel J, Cotgreave IA, Orrenius S and Slater AF (1996) Rapid and specific efflux of reduced glutathione during apoptosis induced by anti-Fas/APO-1 antibody. J. Biol. Chem. 271: 15420–15427.

32. Martensson J, Lai JC and Meister A (1990) High-affinity transport of glutathione is part of a multicomponent system essential for mitochondrial function. Proc. Natl. Acad. Sci. USA 87: 7185–7189.

33. Pearson G, Robinson F, Beers Gibson T, Xu BE, Karandikar M, Berman K and Cobb MH (2001) Mitogen-activated protein (MAP) kinase pathways: regulation and physiological functions. Endocr. Rev. 22: 153–183.

34. Farooq A and Zhou MM (2004) Structure and regulation of MAPK phosphatases. Cell Signal 16: 769–779.

35. Werner E and Werb Z (2002) Integrins engage mitochondrial function for signal transduction by a mechanism dependent on Rho GTPases. J. Cell. Biol. 158: 357–368.

36. Small GW, Shi YY, Edmund NA, Somasundaram S, Moore DT and Orlowski RZ (2004) Evidence that mitogen-activated protein kinase phosphatase-1 induction by proteasome inhibitors plays an antiapoptotic role. Mol. Pharmacol. 66: 1478–1490.

37. Yoon HS and Kim HA (2004) Prolongation of c-Jun N-terminal kinase is associated with cell death induced by tumor necrosis factor alpha in human chondrocytes. J. Korean Med. Sci. 19: 567–573.

38. Mizuno R, Oya M, Shiomi T, Marumo K, Okada Y and Murai M (2004) Inhibition of MKP-1 expression potentiates JNK related apoptosis in renal cancer cells. J. Urol. 172: 723–727.

39. Wang HY, Cheng Z and Malbon CC (2003) Overexpression of mitogen-activated protein kinase phosphatases MKP1, MKP2 in human breast cancer. Cancer Lett. 191: 229–237.

40. Bessede G, Miguet C, Gambert P, Neel D and Lizard G (2001) Efficiency of homocysteine plus copper in inducing apoptosis is inversely proportional to gamma-glutamyl transpeptidase activity. Faseb J. 15: 1927–1940.

41. Tan S, Schubert D and Maher P (2001) Oxytosis: a novel form of programmed cell death. Curr. Top. Med. Chem. 1: 497–506.

42. Tan S, Sagara Y, Liu Y, Maher P and Schubert D (1998) The regulation of reactive oxygen species production during programmed cell death. J. Cell Biol. 141: 1423–1432.

43. Dorfman K, Carrasco D, Gruda M, Ryan C, Lira SA and Bravo R (1996) Disruption of the erp/mkp-1 gene does not affect mouse development: normal MAP kinase activity in ERP/MKP-1-deficient fibroblasts. Oncogene 13: 925–931.

44. Wong SH, Knight JA, Hopfer SM, Zaharia O, Leach Jr CN and Sunderman Jr FW (1987) Lipoperoxides in plasma as measured by liquid-chromatographic separation of malondialdehyde-thiobarbituric acid adduct. Clin. Chem. 33: 214–220.

45. Tormos C, Javier Chaves F, García MJ, Garrido F, Jover R, O'Connor JE, Iradi A, Oltrá A, Oliva MR and Sáez GT (2004) Role of glutathione in the induction of apoptosis and c-fos and c-jun mRNAs by oxidative stress in tumor cells. Cancer Lett. 208: 103–113.

46. Brigelius R, Muckel C, Akerboom TP and Sies H (1983) Identification and quantitation of glutathione in hepatic protein mixed disulfides and its relationship to glutathione disulfide. Biochem. Pharmacol. 32: 2529–2534.

47. Navarro J, Obrador E, Pellicer JA, Aseni M, Viña J and Estrela JM (1997) Blood glutathione as an index of radiation-induced oxidative stress in mice and humans. Free Radic. Biol. Med. 22: 1203–1209.

48. Hissin PJ and Hilf R (1976) A fluorometric method for determination of oxidized and reduced glutathione in tissues. Anal. Biochem. 74: 214–226.

49. Jorge R, Zarich N, Oliva JL, Azanedo M, Martinez N, de la Cruz X and Rojas JM (2002) HSos1 contains a new amino-terminal regulatory motif with specific binding affinity for its pleckstrin homology domain. J. Biol. Chem. 277: 44171–44179.

50. García-Bernal D, Wright N, Sotillo-Mallo E, Nombela-Arrieta C, Stein JV, Bustelo XR and Teixidó J (2005) Vav1 and Rac control chemokine-promoted T lymphocyte adhesion mediated by the integrin $\alpha 4 \beta 1$. Mol. Biol. Cell. 16: 3223–3235.